scientific reports

OPEN

Power supply characterization of baseload and flexible enhanced geothermal systems

Mohammad J. Aljubran✉ & Roland N. Horne

We investigated the techno-economic feasibility and power supply potential of enhanced geothermal systems (EGS) across the contiguous United States using a new subsurface temperature model and detailed simulations of EGS project life cycle. Under business-as-usual scenarios and across depths of 1–7 kilometers, we estimated 82,945 GW and 0.65 GW of EGS supply capacity with lower levelized cost of electricity than conventional hydrothermal and solar photovoltaic projects, respectively. Considering the scenario of flexible geothermal dispatch via wellhead throttling and power plant bypass, these estimates climbed up to 184,112 GW and 44.66 GW, respectively. The majority of EGS supply potential was found in the Western and Southwestern regions of the United States, where California, Oregon, Nevada, Montana, and Texas had the greatest EGS capacity potential. With advanced drilling rates based on state-of-the-art implementations of recent EGS projects, we estimated an average improvement of 25.1% in the levelized cost of electricity. These findings underscored the pivotal role of flexible operations in enhancing the competitiveness and scalability of EGS as a dispatchable renewable energy source.

Keywords Enhanced geothermal systems, Power, Flexible, Techno-economics

Derived from the Earth's natural heat, geothermal energy is a clean and reliable resource for power generation[1,2]. Conventional geothermal systems (i.e., hydrothermal) are relatively rare and geographically limited as they require the natural co-occurrence of high temperature, in-situ fluid for heat transport, and permeable/fractured rock for fluid flow. Although the United States is the leading country in conventional geothermal power generation, it only represents 0.4% of the nationwide electricity generation[3]. Recent technological advancement and field implementation successfully have demonstrated Enhanced Geothermal Systems (EGS) in which heat transport and fluid flow are supplemented artificially by water injection and rock stimulation, respectively[4]. EGS are applicable across geographies, as naturally elevated subsurface temperatures are always present across depths[5]. As a zero-carbon and small-footprint technology[6], EGS represent a promising contender for cost-effectively decarbonizing electricity grids. Hence, conducting a comprehensive techno-economic analysis is useful to estimate the supply potential, economic viability, and geographical favorability of EGS.

Several studies evaluated the long-term value and deployment potential of EGS power using capacity expansion modeling[7–9]. These efforts were based on EGS supply potential estimates from prior work[5,10–12]. Blackwell et al.[10] estimated that only 2% of EGS resources across depths of 3–10 km in the contiguous United States could yield energy 2500 times greater than the 2006 United States energy consumption. Augustine et al.[8] and Lopez et al.[12] estimated that EGS technology has a potential power generation capacity of 7497 GW and 4000 GW, respectively. These estimates were primarily governed by multiple factors: accuracy of subsurface temperature predictions, reservoir temperature decline rate over time, heat-to-power conversion efficiency, and granularity of EGS project life cycle simulations.

First, these earlier studies used a semi-analytical temperature-at-depth model originally developed for the contiguous United States by researchers at Southern Methodist University (SMU) Geothermal Laboratory as part of a 2006 study on *The Future of Geothermal Energy*[7,10,13]. Because the SMU model only spanned depths of 3.5–10 km, other studies on capacity expansion modeling[9] incorporated another temperature-at-depth model developed by researchers at the National Renewable Laboratory (NREL) to cover the shallower depths of 0–3 km[14]. This model was a kriging-based extrapolation of the 3.5–10 km SMU temperature-at-depth model. However, the SMU and NREL models are inadequate in several regards, e.g., low spatial resolution, dismissal of areas with

Energy Science and Engineering, Stanford University, Building 367, Stanford, California 94305, USA. ✉email: aljubrmj@stanford.edu

convective upflow, amongst others[15]. Specifically, comparing the 3 km and 3.5 km layers of the NREL and SMU models showed that temperature-at-depth decreases on average by nearly 40 °C over a short interval of 0.5 km; hence, they were inconsistent with the understanding that temperature generally increases with depth. Second, these studies assumed a fixed annual reservoir decline rate. For instance[8], assumed a fixed thermal decline rate of 0.3%. Third, in estimating the heat-to-power conversion efficiency, they assumed that efficiency was a discrete function of the reservoir temperature only (i.e., one efficiency value for each reservoir temperature range of 25 °C), with no regard to the spatiotemporal variations in ambient temperature. Fourth, the aforementioned studies on EGS supply characterization performed techno-economic modeling using Geothermal Electricity Technology Evaluation Model (GETEM)[16], which is limited to annual timesteps, fixed linear annual reservoir temperature decline, fixed ambient temperatures, and baseload operations.

In this study, we improved the estimates of EGS supply potential across the contiguous United States by developing a new temperature-at-depth model and incorporating more accurate time-dependent and weather-dependent simulations of the EGS project life cycle. Our new thermal Earth model for the contiguous United States was developed using an interpolative physics-informed graph neural network, which was trained to comply approximately with Fourier's Law of heat conduction in the subsurface[17,18,18,19]. We also incorporated a detailed EGS life cycle simulator, called Flexible Geothermal Economics Modeling (FGEM)[20]. Using these models, we evaluated the spatial availability and economics of EGS in the United States. Two drilling rate scenarios were considered: baseline and advanced drilling. The advanced drilling scenario accounted for the improved performance in drilling rates (i.e., decrease in drilling costs) as observed in recent field implementations of EGS projects[21]. Additionally, we investigated the optimal depths required to maximize the economic outlook of EGS across the contiguous United States. Considering baseload and flexible operations, we estimated the EGS supply potential with respect to capital cost and the levelized cost of electricity (LCOE). We also investigated seasonal generation variability of flexible operations to evaluate its effectiveness in improving the EGS project economics for developers and reducing carbon emissions for system operators.

Main
Thermal Earth model
We developed the Stanford Thermal Model (STM) using interpolative physics-informed graph neural networks, over 400,000 bottomhole temperature measurements, and other physical quantities such as depth, geographic coordinates, elevation, sediment thickness, magnetic anomaly, gravity anomaly, gamma-ray flux of radioactive elements, seismicity, electric conductivity, and proximity to faults and volcanoes[15]. STM spanned depths of 0–7 km at an interval of 1 km with spatial resolution of 18 km^2 per grid cell. This spatial resolution was sufficient, as a typical 250 MW EGS plant requires about 5–10 km^2 of reservoir planar area to accommodate the thermal resource needed, assuming that heat removal occurs over a reservoir thickness of 1 km at depth[7]. Evaluated on 40,000 hold-out bottomhole temperature measurements, STM scored a temperature prediction accuracy of 6.4 °C, a nearly ten-fold improvement over the SMU and NREL models. STM closely complied with the three-dimensional Fourier's Law of heat conduction with mean absolute error of 0.7 mW/m^2, and resulted in nondecreasing temperatures with depth almost everywhere. Using Monte Carlo Dropouts[22,23], we found that STM had an average model uncertainty of 9.6% in predicting temperature-at-depth across the contiguous United States.

To verify the model performance and demonstrate its utility, we visualized the spatial variation in predictions of our model compared to the NREL and SMU model. The NREL model was originally developed using linear extrapolation of the SMU predictions at 3.5 km coupled with residual kriging. As seen in Fig. 1, our predictions of subsurface temperature were visualized as heat maps across depths, overlain by isotherms based on the NREL predictions. The NREL model showed spatially circular/Gaussian patterns as it was based on kriging, involving a Gaussian process regression. Kriging is a minimum curvature algorithm with the tendency to overestimate or underestimate areas sparsely populated with measurements. This effect prevailed in highly convective ares, where the NREL model overestimated temperature across extended regions, such as the Great Basin.

Similarly, we visualized the spatial variation in predictions of our model compared to the SMU model. As seen in Fig. 1, our predictions of subsurface temperature were visualized as heat maps across depths, overlain by isotherms based on the SMU predictions. Our model predictions revealed a significant concentration of high-temperature zones in the western United States, aligning with the red isotherms of the SMU model, thus verifying the high-temperature predictions of both models in these regions. According to our model, the central and eastern United States generally displayed lower temperature gradients, which again corresponded with the blue isotherms indicating lower temperatures in the SMU model. Multiple high-temperature geological features were captured by both models, such as Northern and Central Rocky Mountains, Basin and Ridge, Imperial Valley, Yellowstone caldera, Valles caldera, Newberry caldera, Coastal Plains (Western Gulf), amongst others. Also, several low-temperature areas were captured by both models, such as Black Hills, Low Western Plains, San Joaquin Valley, amongst others. However, we observed that the SMU model generally underestimated temperature across depths compared to our model. Examples of areas with underestimated temperature predictions were the Northern and Southern Pacific Coast Ranges, Texas Coastal Plain (Western Gulf), Appalachian Plateau, amongst others. These differences were attributed to variations in the underlying datasets, modeling approaches, and assumptions used in each model.

Furthermore, we compared temperature-at-depth predictions across the Great Basin from our model and the USGS model recently developed by Burns et al.[25]. The average temperature predictions for both models were visualized across depths, along with the individual site predictions from our model in gray. The average temperature profile from our model showed a higher temperature across all depths compared to the USGS model. Whereas the USGS model was linear, our model followed Fourier's Law, resulting in concave temperature predictions across depths. Consequently, the differences in predictions between the two models were, on average, smaller closer to
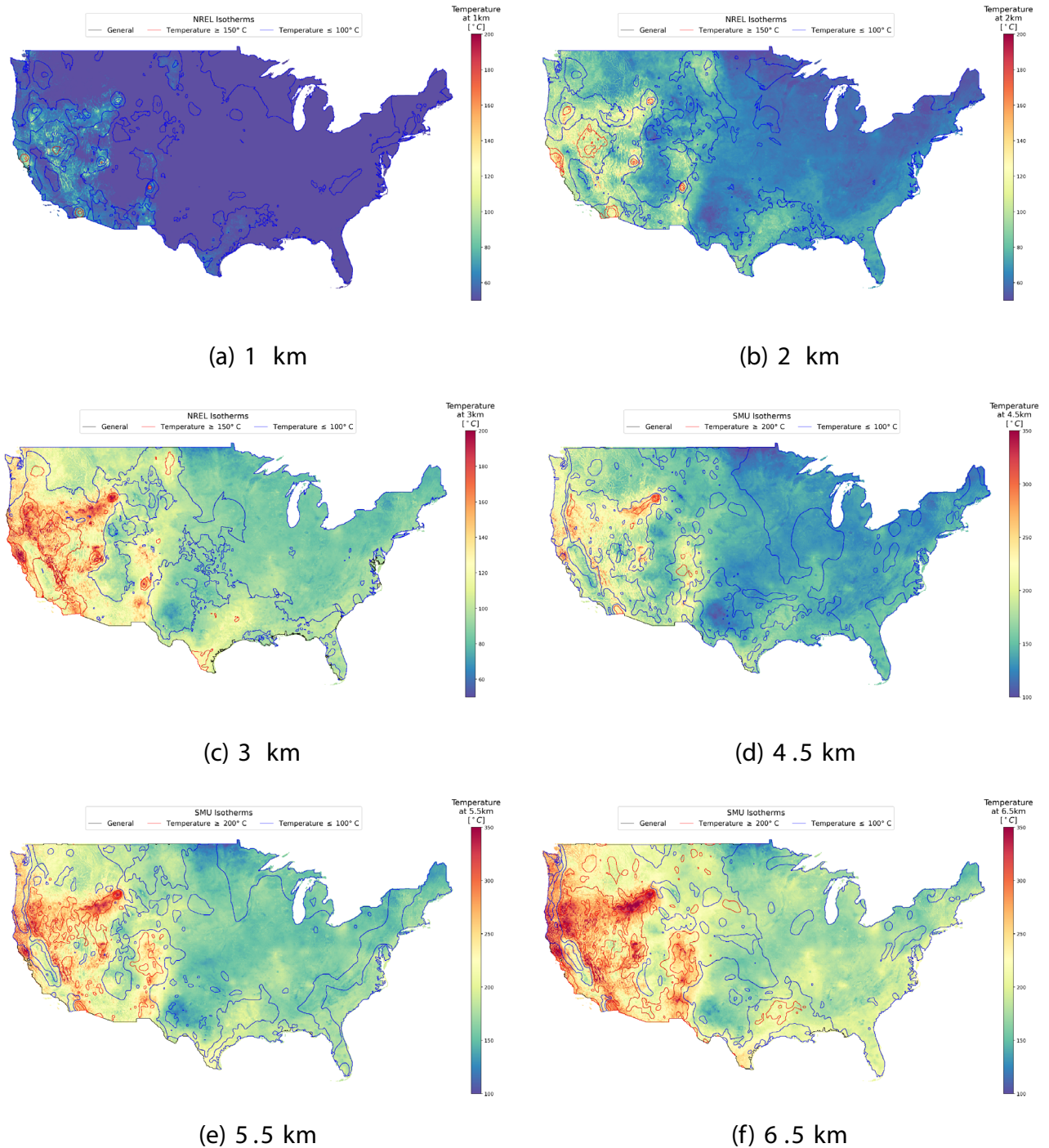
Figure 1. Temperature-at-depth heatmap of our model predictions overlain by isotherms based on the predictions by the NREL and SMU models across depth intervals of 1–3 km and 4.5–6.5 km, respectively. This figure was created using Python 3.9[24].

the surface and around 7 km. We observed a considerable variability in our predicted temperature profiles across sites, indicating a wide range of subsurface temperatures across the Great Basin. Furthermore, as seen in Fig. 2, we visualized the spatial distribution of prediction differences of the USGS model by Burns et al.[25] minus our model across the Great Basin. Although they demonstrated close temperature predictions on average at shallow depths, the spatial distribution showed various locations with temperature differences up to 100 °C. These plots show a strong trend where our model resulted in greater predictions closer to the periphery of the Great Basin. Burns et al.[25] noted that their depth-to-basement model, which was an important input to their temperature model for the Great Basin, was only reliable away from the periphery. Also, our model showed lower temperature predictions on average around the center of the Great Basin, with magnitudes increasing with depth. We
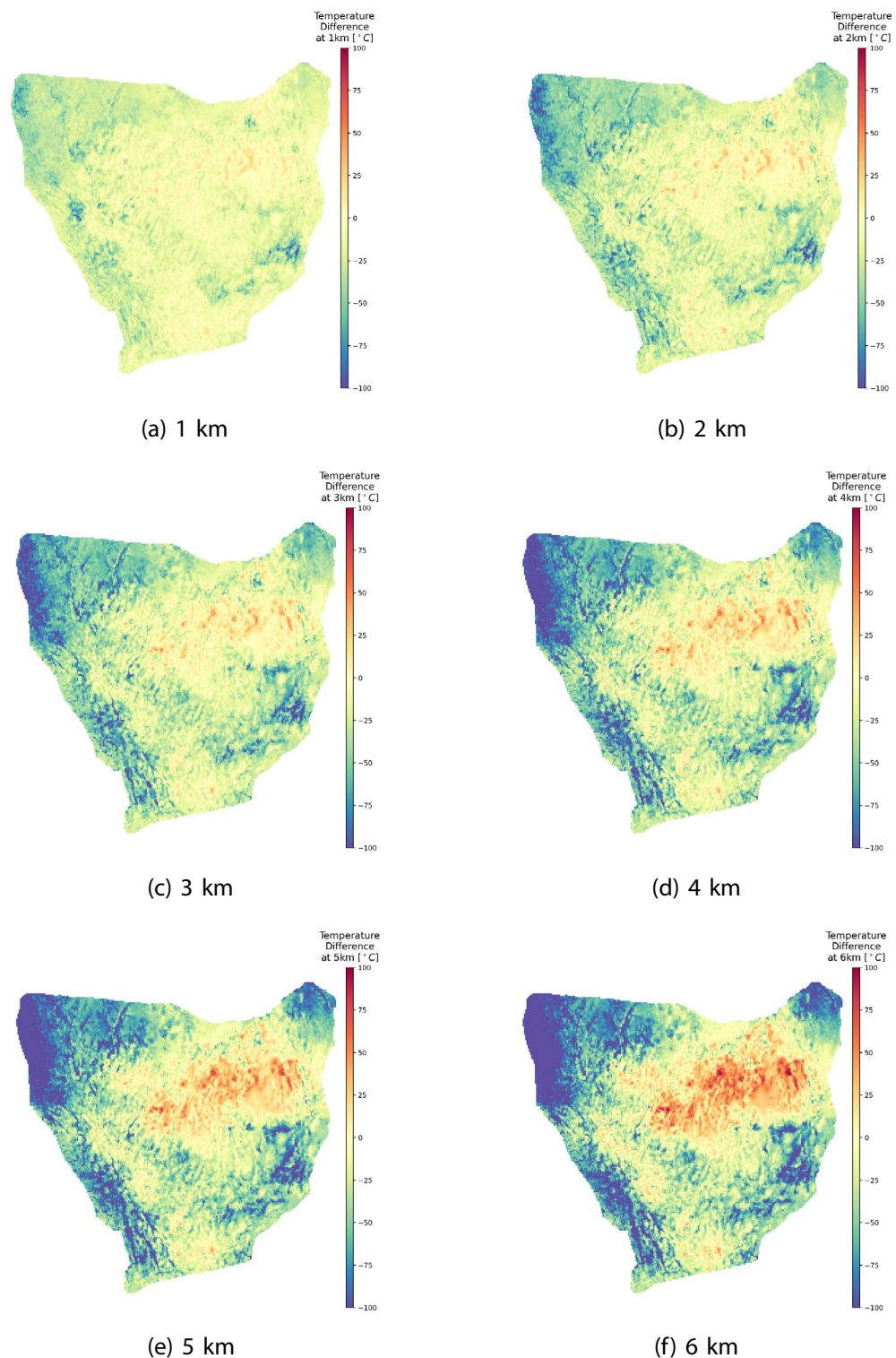
Figure 2. Difference of temperature-at-depth predictions of the USGS model by Burns et al.[25] minus our STM model across the Great Basin. This figure was created using Python 3.9[24].

attributed the differences between these models to the variations in the datasets used, calibration methods, and underlying assumptions about thermal properties and heat flow mechanisms.

Using the STM predictions of temperature-at-depth, we estimated the recoverable heat-in-place. Following other studies[10], we assumed a heat recovery factor, rock density, and rock heat capacity of 2%, 2550 kg/m^3, and 1 kJ$_{th}$/kg–C, respectively. Additionally, we only considered resources with reasonably high temperature-at-depth of 100 °C or higher. STM yielded total recoverable thermal energy of 327×10^{24} J$_{th}$. In particular, thermal energy

attainable is 15×10^{24} J$_{th}$ and 312×10^{24} J$_{th}$ across depth intervals of 1–3 km and 4–7 km, respectively. Previously, the NREL and SMU model estimates were 47×10^{24} J$_{th}$ and 108×10^{24} J$_{th}$ across depth intervals of 1–3 km and 4–7 km, respectively. Across the respective depth intervals, our estimates were approximately three times smaller than the NREL estimates and three times larger than the SMU estimates. These differences were attributed to variations in the underlying datasets, modeling approaches, and assumptions across models. Particularly, the NREL model was based on kriging which is a minimum curvature algorithm that yields smooth surfaces following a Gaussian distribution, hence it tends to overestimate highly convective zones[14,26].

Nationwide resource capacity potential

We performed techno-economic analysis on each 18 km^2 grid cell of STM across depths of 1–7 km to evaluate the EGS resource capacity. We assumed that EGS resources across the United States would be exploited through multiple independent projects, each operating on an 18 km^3 lease (i.e., 18 km^2 in areal extent and 1 km in thickness). To simulate the life cycle of EGS plants, we used FGEM which is an integrated sequential model for end-to-end techno-economic representation of both subsurface and surface geothermal power system components (e.g., subsurface reservoir, production and injection wellbores, power plant, weather). In addition to baseload operations, FGEM is also capable of simulating flexible geothermal operations through wellhead throttling and power plant bypass. Following the designs and operational parameters of successful EGS implementations[21,27–29], we considered EGS doublets of horizontal production and injection wells each with a 2000-meter lateral section completed with 9.625 inch casing strings. Each doublet was set to occupy a hydraulically stimulated reservoir with 1.16 km^3 bulk volume and 10% porosity, seen in Fig. 3. A total of 16 doublets were required to fill in each 18 km^2 grid cell. Each well was set to flow 125 kg/s, which was the target flow rate set by NREL and DOE in the recent Enhanced Geothermal Shot study[8]. The EGS reservoir was modeled as a single-continuum represented by a system of partial differential equations describing a transient convection-diffusion semi-infinite system. We assumed the use of Organic Rankine Cycle (ORC) power plants, which offer zero-emission and promising means for heat-to-power conversion in applications such as EGS[30]. We considered an EGS project lifetime of 25 years. All financial quantities reported in this article were based on 2023 dollars.

Accounting for parasitic power losses (e.g., production and injection pumping requirements), we estimated the potential of EGS capacity across the contiguous United States. Following Augustine et al.[8], we only considered resources with techno-economically significant for power generation with temperature-at-depth of 150 °C or higher. Considering baseload operations, Fig. 4 shows the spatial distribution of the aggregate EGS generation capacity over the project lifetime. Considering EGS resource development spanning depths of 1–7 km across the contiguous United States and excluding sites with barriers to development (e.g., biological resources, environmental sensitivity, urban areas, cultural and tribal land), we estimated the annual net generation potential to be nearly 309 times greater than the 2023 United States power consumption of 4014 TWh. It is important to note that 78% of that potential was at depth of 6–7 km, where subsurface temperatures were significantly high compared to shallower depths. We estimated a total gross EGS capacity potential of 245,032 GW, significantly greater than the most recent estimates of 7469 GW by Augustine et al.[8], which we attributed to multiple factors. Previous studies relied on the SMU maps which predicted temperatures to be, on average, 29.3% smaller across depths compared to our model, as seen in Fig. 1. Also, Augustine et al.[8] assumed that the EGS power potential per rock volume was in the range of 0.59–1.19 MW/km^3 for resource temperatures of 150–350 °C. This was an order of magnitude lower than practical observations which indicate that a 210 °C reservoir, for instance, has a
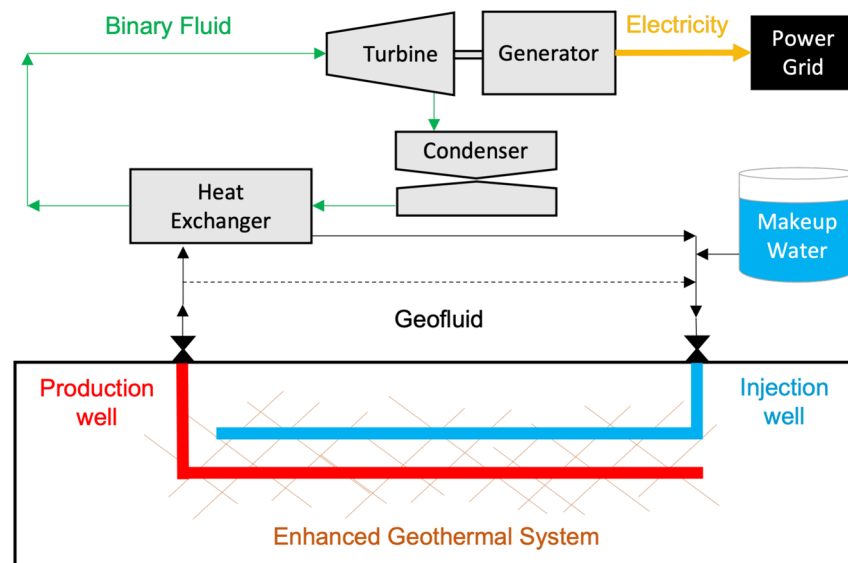

Figure 3. Configuration of an EGS project with a single production-injection doublet, ORC binary power plant, plant bypass line, makeup water source, and power grid connection.
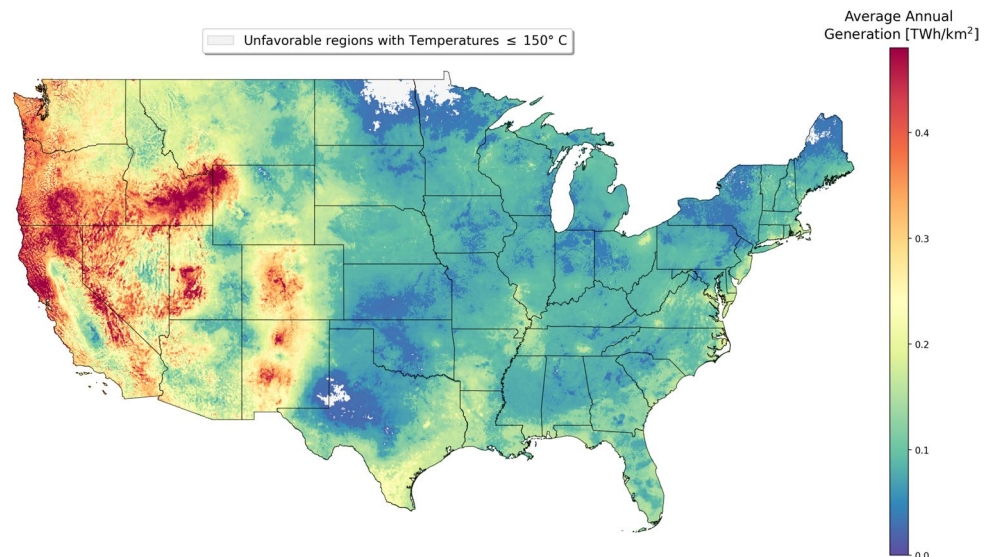
Figure 4. Spatial distribution of average annual generation per unit area across for projects spanning depths of 1–7 km. Grey areas indicate techno-economically infeasible locations, with temperature-at-depth of < 150 °C at a depth of 7 km. This figure was created using Python 3.9[24].

power density of nearly 10 MW/km[37,31]. Our techno-economic modeling results indicated a nationwide average of 11 MW/km^2 across depths, which was more aligned with practical observations. Although the estimated EGS power potential is large, it is important to note the amount that can be economically produced is likely to be much smaller.

Figure 4 shows that the majority of EGS net generation potential per unit area is in the Western and Southwestern regions of the United States. After excluding sensitive land, California showed the greatest capacity potential for EGS, with a total capacity potential of 20,882 GW. Oregon, Nevada, Montana, and Texas followed in rank with relatively high potential of 18,270, 16,484, 15,681, and 14,578 GW, respectively. Generally, high-capacity locations were observed around volcanic and thermally active areas, such as Valles Caldera in New Mexico, La Garita Caldera in Colorado, Newberry Volcano in Oregon, the Great Basin, The Geysers in California, Coso Volcanic Field in California, Salton Buttes in California, amongst others.

Techno-economics of EGS projects

Beyond the distribution of EGS resource capacity, we also evaluated the economic viability for each 18 km^3 EGS project based on capital expenditure (CAPEX), operational expenditure (OPEX), and generation over time, which were represented in terms of LCOE with a discount rate of 7% and investment tax credit (ITC) of 30%, following the 2022 United States Inflation Reduction Act. Considering the business-as-usual (BAU) scenario of baseload dispatch and baseline drilling rates, the optimal (i.e., minimum) LCOE across depths of 1–7 km was computed for each 18 km^2 project location, seen in Fig. 5. We found that for 89.3% of the United States areal extent, LCOE was minimized by drilling to the deepest point, i.e., 7 km. Meanwhile, drilling to depths of ≤ 4 km was found optimal only across 0.27% of the United States areal extent, mainly around Western United States. This was attributed to the decreasing geothermal gradients in such areas, where the increasing drilling costs with depth did not justify the associated benefits of increased EGS resource temperature. Advanced drilling rates were based on recently observed drilling learning curves in EGS projects, where drilling costs dropped by nearly 50% after drilling around three wells[21]. As seen in Fig. 5, considering advance drilling rates resulted in 24.3% LCOE improvement, on average, where the baseline and advanced scenarios resulted in average LCOE of 86.1 and 63.4 USD/MWh, respectively.

We considered various scenarios based on EGS plant dispatch strategy (baseload vs. flexible) and drilling rates (baseline vs. advanced), seen in Fig. 6. Additionally, we compared our EGS supply curve estimates to other renewables as reported in the 2023 Annual Technology Baseline (ATB) by NREL[32]. Based on industry standards, the 2023 NREL ATB assumed nominal discount rates in the range of 6–8% across different energy resources. For each resource, they assumed the techno-economically optimal choice of 30% investment tax credit and 27.5 USD/MWh production tax credit. Throughout this study, we used 7% nominal discount rate and 30% ITC to evaluate EGS economics.

The 2023 NREL ATB reported that recent signings of geothermal power purchase agreements (PPAs) in the United States had an average pricing of 70 USD/MWh. Considering the BAU scenario of baseload dispatch and baseline drilling costs, a total of 93,176 GW EGS resource capacity was available with LCOE below that of the average geothermal PPA pricing. EGS falls under the umbrella of dispatchable technologies with the capability of varying power output based on demand for electricity[32]. Other naturally and commonly dispatchable renewable resources include hydrothermal and biomass, with LCOE estimates of 67.2 USD/MWh and 90.2 USD/MWh, respectively. Compared to LCOE estimates of hydrothermal and biomass resources, we estimated a total
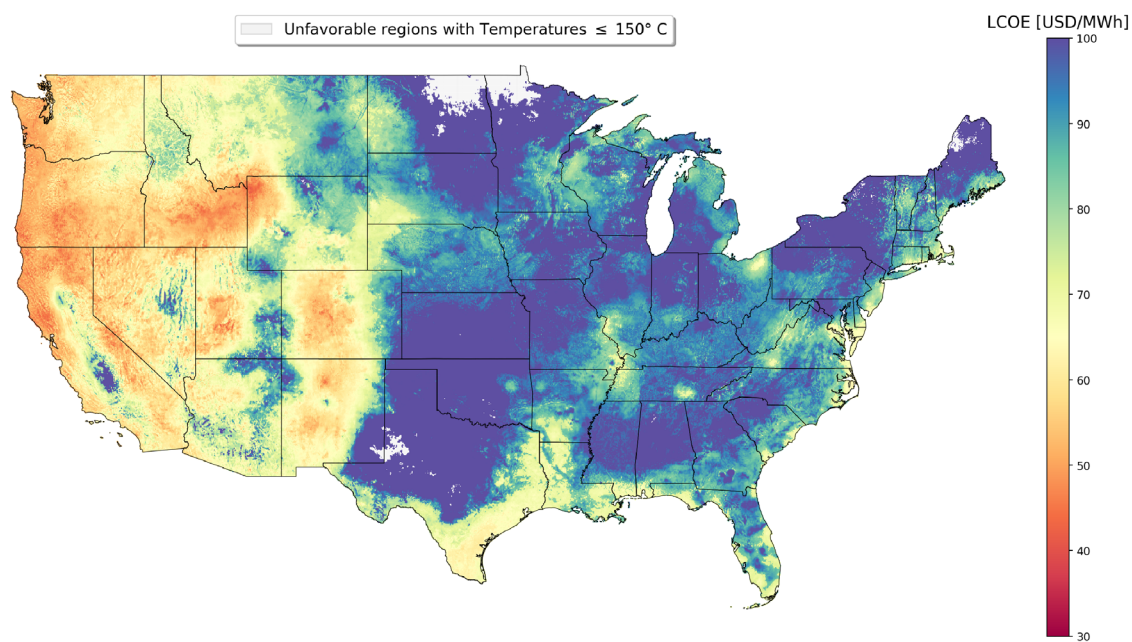
(a) Baseline Drilling Rates
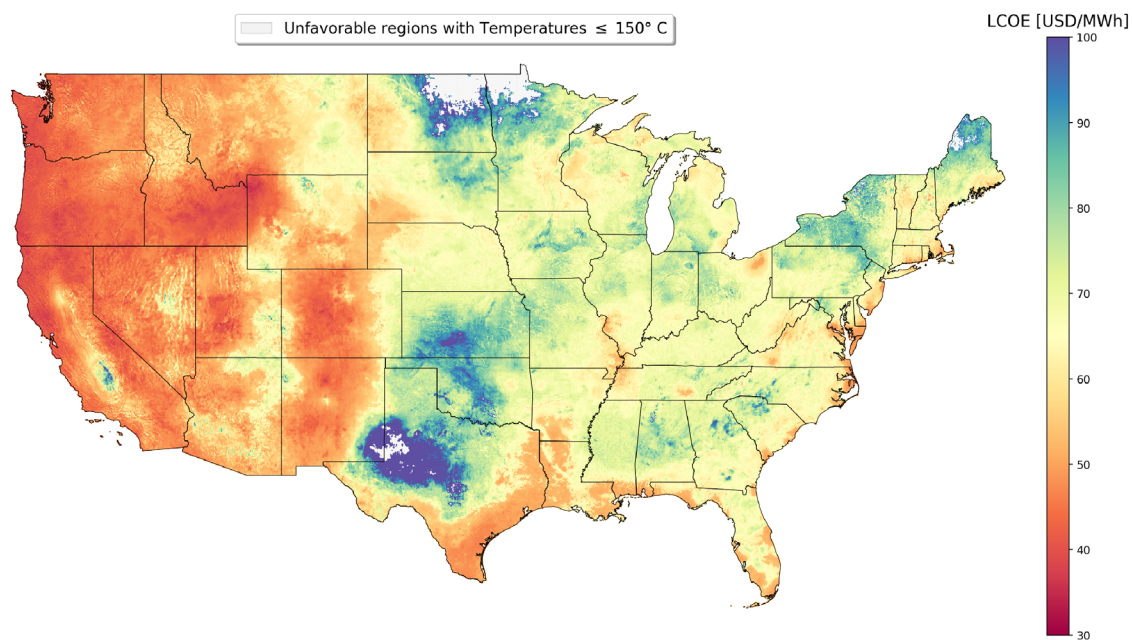
(b) Advanced Drilling Rates

Figure 5. Optimal LCOE across depths for EGS development across the contiguous United States, under baseload dispatch scenario with (**a**) baseline and (**b**) advanced drilling rates. Grey areas indicate techno-economically infeasible locations, with temperature-at-depth of < 150 °C at the deepest reservoir zone of 7 km. This figure was created using Python 3.9[24].

EGS resource capacity under BAU scenario of 82,945 GW and 155,821 GW, respectively. Solar photovoltaic (PV) resources can be made dispatchable at an LCOE of 80.7 USD/MWh when augmented with Lithium-ion battery storage[32]. Under such marginal LCOE pricing, our estimates indicated a total EGS resource capacity of
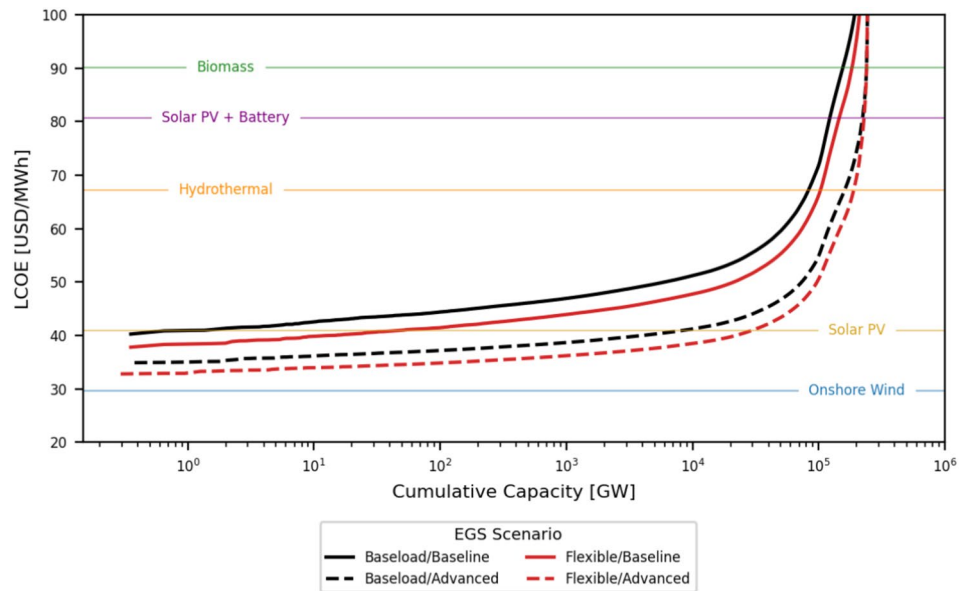
Figure 6. EGS capacity supply curves versus after-ITC LCOE across different operational and drilling cost scenarios, in comparison to the average LCOE of other renewables.

122,569 GW. Other renewables offer resource-constrained (i.e., intermittent) power generation profiles, such as solar PV and onshore wind, but they are characterized with very competitive LCOE of 40.9 USD/MWh and 29.7 USD/MWh, respectively. We estimated total EGS resource capacities of 0.65 GW were economically feasible compared to the marginal LCOE of solar PV, but no EGS resources were found viable compared to onshore wind in terms of LCOE.

We also evaluated the techno-economics of flexible EGS operations where power output was varied to maximize power generation over the project lifetime. We achieved flexible operations using the wellhead throttling and power plant bypass options in FGEM. In particular, we note that the power plant efficiency drops with increasing ambient temperatures and/or decreasing inlet temperature (equivalently, declining subsurface reservoir temperature). Thus, we implemented a controller to allow for increased flow rates, up to 30% of the EGS project design, to maintain power generation as high as possible throughout the lifetime of the project. Figure 7 shows a sample simulation of baseload versus flexible operations simulated at an hourly resolution for an EGS in Nevada targeting a 175 °C resource at a vertical depth of 2 km. Our flexible controller responds to both diurnal and seasonal variations in ambient temperature to maximize the utilization of the power plant installed capacity. Note that increased geofluid production flow rates were associated with greater pumping requirements due to the elevated wellbore pressure drops. Seen in Fig. 7, flexible operations were favorable and yielded 6.36% average reduction in LCOE across EGS resources. Multiple dynamics governed these changes, primarily the average increase of 26 °C in reservoir temperature decline due to increased well flow rates under flexible operations compared to baseload operations. We estimated total flexible EGS resource capacities of 189,667 GW and 46.16 GW that were economically feasible considering the marginal LCOE of biomass and solar PV, respectively.

Considering CAPEX components of an EGS project with extended laterals, EGS drilling costs are the most significant[33]. We found that drilling CAPEX represented an average of 56.2% of the total EGS upfront expenditure across projects. In addition to the baseline drilling rate estimates in FGEM, we also considered advanced scenarios where drilling costs would drop by 50% based on the actual drilling learning curves observed in recent EGS field implementations in Nevada and Utah[21]. In the scenario of flexible operations, adopting advanced drilling rates resulted in an overall LCOE reduction of 25.1% on average. Under flexible operations, we found that advanced drilling rates yielded totals of 239,732 GW and 29,141 GW EGS supply capacities that would be economically feasible compared to the marginal LCOE of biomass and solar PV, respectively.

Recalling the 2023 national United States generation capacity of 1,300 GW, our estimates indicated that EGS development could be a cost-effective dispatchable option that is even competitive with constrained-resource technologies. Additionally, considering the scenario of flexible operations and advanced drilling rates, feasible EGS prospects with LCOE less than 70 USD/MWh were often deeper underground. Specifically, depths of 1–3 km, 4–5 km and 6–7 km represented 1.6%, 24.7% and 73.7%, respectively. With drilling costs increasing parabolically with depth[34], EGS development at scale could be CAPEX-intensive. Figure 8 shows generation capacity supply costs with respect to CAPEX, across target drilling depths and in comparison to other renewables. We found that EGS under flexible operations and advanced drilling rates could yield 49,450 GW of generation capacity with overnight CAPEX of less than or equal to that of the rare conventional geothermal systems (i.e., hydrothermal). Of that generation capacity, 38% were at the industry-standard drilling depths of 1–4 km, while the remaining required tapping into deeper reservoir zones. Therefore, drilling deeper is key to unlocking prolific and cost-effective EGS resources.
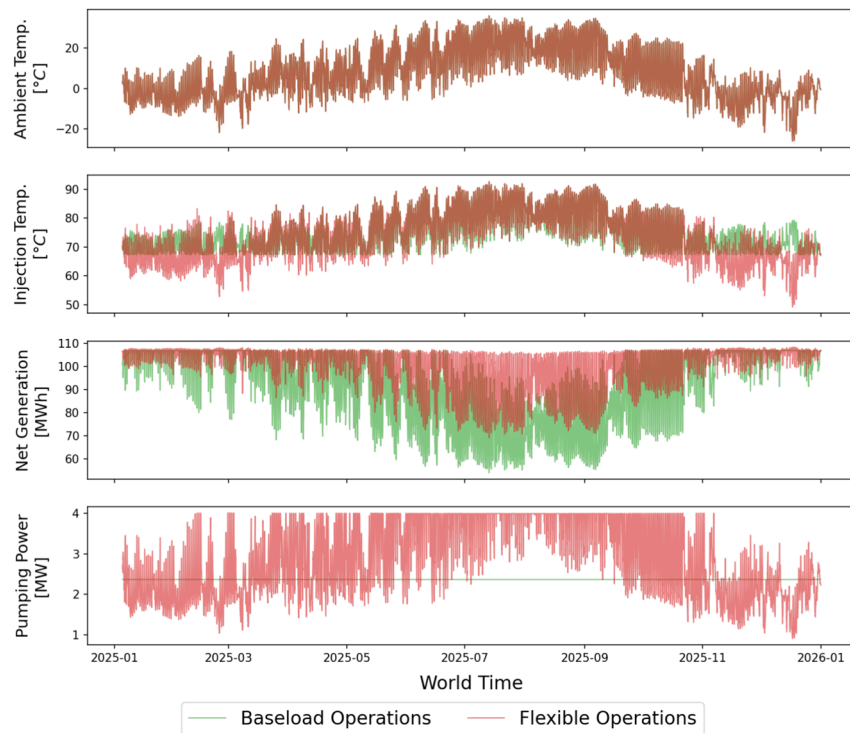
Figure 7. Sample of annual baseload versus flexible operations in green and red, respectively, of an EGS project simulated at an hourly resolution using FGEM. Brown curves indicate overlapping baseload and flexible profiles.
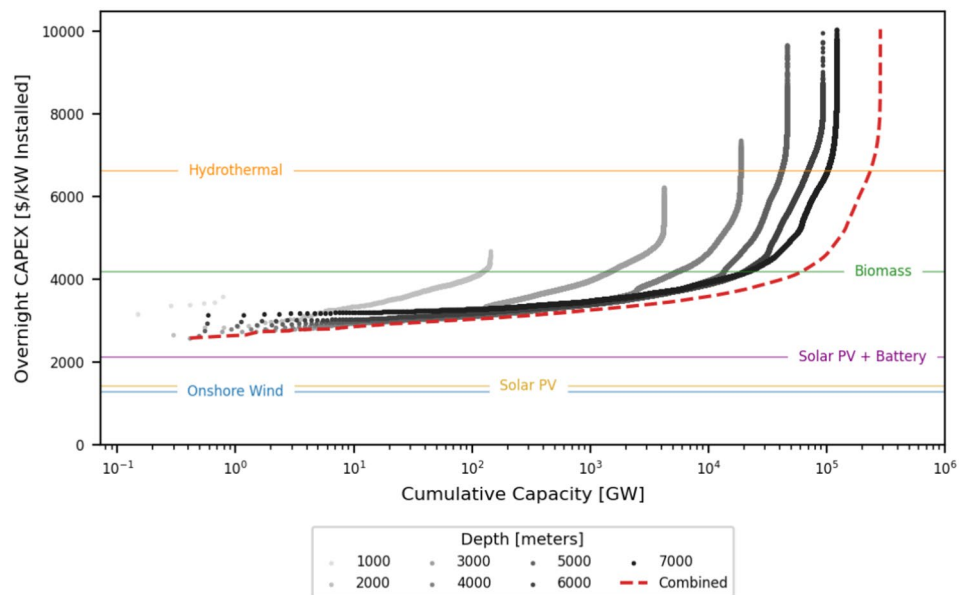

Figure 8. EGS capacity supply curves versus before-ITC overnight CAPEX across target reservoir depths for the scenario of flexible operations and advanced drilling costs, in comparison to the average CAPEX of other renewables.

Discussion

In this work, we presented STM, a thermal model for the upper crust of the contiguous United States to evaluate geothermal resources. We leveraged interpolative physics-informed graph neural networks and integrated a rich dataset comprising over 400,000 bottomhole temperature measurements and diverse geophysical parameters, including sediment thickness, magnetic and gravity anomalies, and seismicity. This model achieved state-of-the-art granularity and accuracy, with a spatial resolution of 18 km^2 per grid cell and coverage spanning depths

of 1–7 km at 1 km intervals. Compared to other industry-standard models developed by SMU[10] and NREL[14], STM showed a ten-fold improvement in mean absolute error in comparisons with actual (hold-out) well temperature measurements. STM also involved elevated surface heat flow predictions across the Western United States, largely due to the presence of the Pacific Ring of Fire, where tectonic movements favor volcanic activities and geothermal heat transfer. In particular, multiple locations stood out, such as Yellowstone in Wyoming, Basin and Range Province extending mainly across Nevada and neighboring states with thinner crustal thickness, the Cascade Range starting from northern California and reaching to British Columbia, Canada and including active volcanoes like Mount St. Helens and Mount Rainier, Coso Volcanic Field in California, Rio Grande Rift stretching from New Mexico to Colorado, and Imperial Valley in California partly due to the San Andreas Fault system. Away from the Western flank, elevated surface heat flow values were also observed in the Appalachian Mountains and along the Gulf Coast.

The results of our techno-economic analysis revealed a huge EGS resource potential across the contiguous United States, surpassing previous estimates. With a total potential capacity of 35,808 GW, our findings underscored the significant role that EGS could play in meeting future energy demands. Notably, the majority of this potential was concentrated in the Western and Southwestern regions of the United States, with Texas, California, Oregon, and Nevada being the most prolific states for EGS development. These areas coincided with volcanic and otherwise thermally elevated regions, highlighting the importance of geological factors in determining the suitability of sites for EGS projects. Comparisons with previous estimates highlighted the advantage of the STM model in capturing local heat anomalies and providing more accurate assessments of EGS potential. By considering depths shallower than 3 km and employing a finer spatial resolution, our analysis offered a more comprehensive understanding of the geothermal resources available for exploitation, seen in Fig. 4.

The economic viability of EGS projects depends not only on their resource capacity but also on financial factors such as CAPEX, OPEX, and generation over time, where all govern LCOE. Conducted with a discount rate of 7% and ITC of 30%, our analysis showed that drilling to the deepest point (i.e., 7 km in this study) minimized LCOE across the majority of the United States, encompassing 89.3% of the country's areal extent. However, in certain regions characterized by decreasing geothermal gradients, such as western North Dakota, Snake River Plain, and the Great Basin, drilling to depths of $\leq$ 4 km was found to be optimal, accounting for 0.27% of the nation's areal extent. This highlights the nuanced interplay between geological factors and economic considerations in determining the optimal depth for EGS projects.

Under a BAU scenario, where baseload dispatch and baseline drilling rates were assumed, a substantial portion of EGS resource capacity were cheaper to generate than the 2023 average geothermal PPA pricing of 70 USD/MWh. EGS demonstrated competitive LCOE compared to other dispatchable renewables such as hydrothermal and biomass along with significant supply potential, underscoring its potential as a reliable and scalable renewable resource. Moreover, we found that EGS could be a promising alternative for augmenting resource-constrained and intermittent resources such as PV solar and wind. By implementing wellhead throttling and power plant bypass options in our analysis, we demonstrated the capability of EGS plants to adjust power output dynamically, resulting in an average decrease of 6.36% in LCOE across EGS resources. Our simulations, exemplified by the case of an EGS project in Nevada targeting a 175 °C resource at a depth of 2 km, illustrated the effectiveness of flexible controllers in responding to ambient temperature fluctuations, thereby optimizing the utilization of installed power plant capacity. Notably, the adoption of flexible operations unlocked significant potential for expanding EGS resource capacity, with feasible potential reaching 184,112 GW and 44.66 GW compared to the marginal LCOE of biomass and solar PV, respectively. These findings underscored the pivotal role of flexible operations in enhancing the competitiveness and scalability of EGS as a dispatchable renewable energy source. In addition to considering cost components in designing and operating EGS systems, developers should also evaluate the revenue streams associated with EGS development to ultimately estimate the potential return on investment.

Methods
Stanford thermal model (STM)
With focus on thermal Earth modeling, we previously developed methods for nonlinear spatial interpolation of physical quantities using interpolative physics-informed graph neural networks[15]. In the current study, we deployed these methods to develop an updated thermal Earth model for the contiguous United States, called STM. In particular, we used these methods over a grid consisting of over 400,000 nodes with measured bottomhole temperature and 4,279,536 other nodes where predictions of thermal quantities were desired (i.e., spatial resolution of nearly 18 km^2 across depths of 1–7 km with an interval of 1 km). A directed graph was constructed using nearest neighbors with Euclidean distance, such that each node had five incoming edges, each weighted using the inverse Euclidean distance. Node-level features included subsurface temperature, rock thermal conductivity, surface heat flow, average surface temperature, elevation, sediment thickness, magnetic anomaly, gravity anomaly, Uranium radiation, Thorium radiation, Potassium radiation, seismicity, electric conductivity, and proximity to faults and volcanoes. Note that these measurements had various spatial resolutions, hence they were downsampled/upsampled accordingly to achieve the target spatial resolution. Because bottomhole temperature measurements are typically conducted at depth inside wellbores with circulating fluids, we corrected them using the Harrison correction[35] to account for thermal disequilibrium[36]. Also, laboratory measurements of rock thermal conductivity were conducted at room conditions and had to be corrected to in-situ temperature conditions[37–39].

STM covered the contiguous United States with a spatial resolution of 18 km^2 and spanned depths of 1–7 km with an interval of 1 km[15]. This work was particularly novel in two ways: graph-based interpolation, and physics coupling. Message passing and aggregation operations in graph neural networks allow for exchanging *input feature* information amongst neighboring nodes to allow for dynamically updating the representation of the node-level state across a graph. Our novel approach also allowed for message passing and aggregating the

target feature information (i.e., thermal quantities in our case) amongst neighboring nodes to leverage interpolation. STM also closely approximated Fourier's Law of conductive heat transfer in the upper crust through the integration of physics-informed loss terms in training the graph neural network.

Flexible geothermal economics modeling (FGEM)

In prior work, we developed FGEM to evaluate the techno-economics of geothermal systems with various operational strategies, such as baseload and flexible[20,40,41]. FGEM couples technical, economic, and market modules at either high- or low-frequency timeframes. FGEM incorporates a diverse array of parameters, from geothermal resource and plant design to operational dispatch strategies and power market dynamics. This unique integration yields valuable insights into the viability of flexible geothermal power systems and their harmonization within the existing energy landscape.

The FGEM workflow requires several user inputs, including a configuration file, data files, and a dispatch strategy. Upon input validation, FGEM then performs sequential modeling through distinct modules, each modeling the techno-economic aspects of specific components within the system. These modules include the subsurface reservoir, single-phase wellbore flow dynamics and heat transfer, weather patterns, power plant performance (single flash or binary systems), energy storage units (e.g., thermal and/or electrochemical energy storage technologies), and power market dynamics (e.g., wholesale, capacity, green energy credits, PPA). For various flash and binary power plant types, FGEM captures the effect of hourly variations in ambient temperature, which govern power plant efficiency and injection fluid temperature as seen in Fig. 7.

We used hourly timesteps to capture the effect of ambient temperature, which resulted in elevated computational intensity in simulating millions of EGS projects across the contiguous United States. Previously, we developed an analytical solution to simulate temperature decline over the lifetime of EGS fractured reservoirs under various operational strategies. This model represents a one-dimensional single-continuum semi-infinite transient diffusion-convection problem and allows for variable well flow rates and injection temperatures[42]. This computationally efficient analytical solution was verified for various scenarios against numerical solutions. Additionally, we utilized ambient temperature forecasts with a nominal spatial resolution of 4 km^2 at an hourly frequency, generated based on open-source generative machine learning methods recently developed by[43] at NREL for meteorological modeling. We also adopted FGEM's financial models to estimate project CAPEX, OPEX, and LCOE with a discount rate of 7% and ITC of 30%. In FGEM, we adopted spatially variant transmission line costs[42] based on 2 USD/mile–kW, and 2022 baseline drilling costs as originally developed in GETEM based on actual geothermal drilling projects[34]. The scenario of advanced drilling was based on 2024 drilling costs reported for EGS projects in Nevada and Utah, which indicated a drop in drilling costs by nearly 50%[21].

Ethics approval and consent to participate

This material is the authors' own original work, which has not been previously published elsewhere. This paper is not currently being considered for publication elsewhere. The paper reflects the authors' own research and analysis in a truthful and complete manner. The paper properly credits the meaningful contributions of co-authors and co-researchers. The results are appropriately placed in the context of prior and existing research. All sources used are properly disclosed. All authors have been personally and actively involved in substantial work leading to the paper, and will take public responsibility for its content.

Data availability

LCOE and supply capacity maps for EGS are made publically available as feature layers on ArcGIS at https://arcg.is/H8fbH0.

References

1. Igwe, C. I. Geothermal energy: A review. *Int. J. Eng. Res. Technol. (IJERT)* **10**, 655–661 (2021).
2. Sharmin, T., Khan, N. R., Akram, M. S. & Ehsan, M. M. A state-of-the-art review on for geothermal energy extraction, utilization, and improvement strategies: Conventional, hybridized, and enhanced geothermal systems. *Int. J. Thermofluids*, 100323 (2023)
3. U.S. Energy Information Administration (EIA) monthly energy review. Technical report (June 2023)
4. Kana, J. D., Djongyang, N., Raïdandi, D., Nouck, P. N. & Dadjé, A. A review of geophysical methods for geothermal exploration. *Renew. Sustain. Energy Rev.* **44**, 87–95 (2015).
5. Aghahosseini, A. & Breyer, C. From hot rock to useful energy: A global estimate of enhanced geothermal systems potential. *Appl. Energy* **279**, 115769 (2020).
6. Chandrasekharam, D. Enhanced geothermal systems (EGS) for un sustainable development goals. *Discover Energy* **2**(1), 4 (2022).
7. Tester, J. W. *et al.* The future of geothermal energy. *Massachusetts Inst. Technol.* **358**, 1–3 (2006).
8. Augustine, C., Fisher, S., Ho, J., Warren, I. & Witter, E. *Enhanced geothermal shot analysis for the geothermal technologies office* (Technical report, National Renewable Energy Laboratory (NREL), Golden, CO (United States), 2023).
9. Ricks, W., Voller, K., Galban, G., Norbeck, J. H. & Jenkins, J. D.: The role of flexible geothermal power in decarbonized electricity systems. *Nat. Energy* 1–13 (2024)
10. Blackwell, D. D., Negraru, P. T. & Richards, M. C. Assessment of the enhanced geothermal system resource base of the United States. *Nat. Resour. Res.* **15**, 283–308 (2006).
11. Augustine, C. R., Ho, J. L. & Blair, N. J.: Geovision analysis supporting task force report: Electric sector potential to penetration. Technical report, National Renewable Energy Lab.(NREL), Golden, CO (United States) (2019)
12. Lopez, A., Roberts, B., Heimiller, D., Blair, N. & Porro, G. Renewable energy technical potentials: A GIS-based analysis. Denver (2012)

13. Blackwell, D., Richards, M., Frone, Z., Batir, J., Ruzo, A., Dingwall, R. & Williams, M. Temperature-at-depth maps for the conterminous US and geothermal resource estimates. Technical report, Southern Methodist University Geothermal Laboratory, Dallas, TX (United States) (2011)

14. Mullane, M., Gleason, M., McCabe, K., Mooney, M., Reber, T. & Young, K. R. An estimate of shallow, low-temperature geothermal resources of the United States. Technical report, National Renewable Energy Lab.(NREL), Golden, CO (United States) (2016)

15. Aljubran, M. J. & Horne, R. N. Thermal Earth model for the conterminous United States using an interpolative physics-informed graph neural network. *Geotherm. Energy* **12**(1), 25 (2024).

16. Mines, G. L. *Getem user manual* (Idaho Falls, ID, USA, INL, 2016).

17. Cengel, Y., Cimbala, J. & Turner, R. *EBOOK: Fundamentals of Thermal-Fluid Sciences (SI Units)* (McGraw Hill, 2012).

18. Mareschal, J.-C. & Jaupart, C. Radiogenic heat production, thermal regime and evolution of continental crust. *Tectonophysics* **609**, 524–534 (2013).

19. Jaupart, C., Labrosse, S., Lucazeau, F. & Mareschal, J. Temperatures, heat and energy in the mantle of the earth. *Treat. Geophys.* **7**, 223–270 (2007).

20. Aljubran, M. & Horne, R. N. FGEM: Flexible geothermal economics modeling tool. *Appl. Energy* **353**, 122125 (2024).

21. El-Sadi, K., Gierke, B., Howard, E. & Gradl, C. Review of drilling performance in a horizontal EGS development. In *Proceedings, 49th Stanford Workshop on Geothermal Reservoir Engineering* (2024)

22. Gal, Y. & Ghahramani, Z.: Dropout as a Bayesian approximation: Representing model uncertainty in deep learning. In: *International Conference on Machine Learning* 1050–1059 (PMLR, 2016).

23. Verdoja, F. & Kyrki, V.: Notes on the behavior of MC dropout. arXiv preprint arXiv:2008.02627 (2020)

24. Van Rossum, G. & Drake, F. L. *Python 3 Reference Manual* (CreateSpace, Scotts Valley, CA, 2009).

25. Burns, E., DeAngelo, J. & Williams, C. F.: Updated three-dimensional temperature maps for the Great Basin, USA. In: *Proceedings, 49th Stanford Workshop on Geothermal Reservoir Engineering* (2024)

26. Yamamoto, J. K. Correcting the smoothing effect of ordinary kriging estimates. *Math. Geol.* **37**, 69–94 (2005).

27. Fercho, S., Matson, G., McConville, E., Rhodes, G., Jordan, R. & Norbeck, J. Geology, temperature, geophysics, stress orientations, and natural fracturing in the milford valley, ut informed by the drilling results of the first horizontal wells at the cape modern geothermal project. In *Proceedings, 49th Stanford Workshop on Geothermal Reservoir Engineering* (2024)

28. Norbeck, J. H. & Latimer, T.: Commercial-scale demonstration of a first-of-a-kind enhanced geothermal system. EarthArXiv (2023)

29. Nadimi, S., Forbes, B., Moore, J., Podgorney, R. & McLennan, J. Utah FORGE: Hydrogeothermal modeling of a granitic based discrete fracture network. *Geothermics* **87**, 101853 (2020).

30. Duniam, S. & Gurgenci, H. Annual performance variation of an EGS power plant using an ORC with NDDCT cooling. *Appl. Therm. Eng.* **105**, 1021–1029 (2016).

31. Cumming, W. Resource capacity estimation using lognormal power density from producing fields and area from resource conceptual models; advantages, pitfalls and remedies. In: *Proceedings, 41st Workshop on Geothermal Reservoir Engineering* 7 (2016)

32. National Renewable Energy Laboratory 2023 annual technology baseline. Technical report, National Renewable Energy Laboratory (NREL), Golden, CO (United States) (2023)

33. Yost, K., Valentin, A. & Einstein, H. H. Estimating cost and time of wellbore drilling for engineered geothermal systems (EGS)-considering uncertainties. *Geothermics* **53**, 85–99 (2015).

34. Robins, J. C., Kesseli, D., Witter, E. & Rhodes, G. *2022 GETEM geothermal drilling cost curve update* (Technical report, National Renewable Energy Laboratory (NREL), Golden, CO (United States), 2022).

35. Harrison, W. E., Luza, K. V., Prater, M. L., Cheung, P. K. & Ruscetta, C. Geothermal resource assessment in oklahoma. Technical report (1982)

36. Schumacher, S. & Moeck, I. A new method for correcting temperature log profiles in low-enthalpy plays. *Geotherm. Energy* **8**(1), 27 (2020).

37. Chapman, D. Thermal gradients in the continental crust. *Geol. Soc. Lond.* **24**(1), 63–70 (1986).

38. Abdulagatov, I. M., Emirov, S. N., Abdulagatova, Z. Z. & Askerov, S. Y. Effect of pressure and temperature on the thermal conductivity of rocks. *J. Chem. Eng. Data* **51**(1), 22–33 (2006).

39. Chen, C. *et al.* Effect of temperature on the thermal conductivity of rocks and its implication for in situ correction. *Geofluids* **2021**, 1–12 (2021).

40. Aljubran, M. J., Volkov, O. & Horne, R. N.: Techno-economic modeling and optimization of flexible geothermal operations coupled with energy storage. In *Proceedings, 48th Stanford on Geothermal Reservoir Engineering, Stanford University, Stanford, CA* (2023)

41. Aljubran, M. J. & Horne, R. N. Techno-economics of geothermal power in the contiguous united states under baseload and flexible operations [manuscript in preparation]. *Renew. Sustain. Energy Rev.*

42. Aljubran, M. & Horne, R. Techno-economics of enhanced geothermal systems across the United States using novel temperature-at-depth maps. In *Proceedings, 49th Stanford Workshop on Geothermal Reservoir Engineering* (2024)

43. Buster, G., Benton, B. N., Glaws, A. & King, R. N. High-resolution meteorology with climate change impacts from global climate model data using generative machine learning. *Nat. Energy* 1–13 (2024).

Acknowledgements

Author contributions

M.A. contributed to conceptualization, methodology, implementation and analysis, and writing the first draft. R.H. contributed to conceptualization, research supervision, and reviewing and editing.

Competing interests

The authors declare no competing interests.

Additional information

Correspondence and requests for materials should be addressed to M.J.A.

Reprints and permissions information is available at www.nature.com/reprints.

Publisher's note Springer Nature remains neutral with regard to jurisdictional claims in published maps and institutional affiliations.